Journal Pre-proof

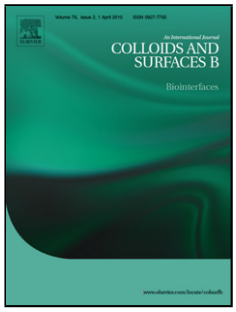

Covalent grafting of titanium with a cathelicidin peptide produces an osteoblast compatible surface with antistaphylococcal activity

Gerard Boix-Lemonche, Jordi Guillem-Marti, Francesca D'Este, José María Manero, Barbara Skerlavaj

PII: S0927-7765(19)30730-1

DOI: https://doi.org/10.1016/j.colsurfb.2019.110586

Reference: COLSUB 110586

To appear in: *Colloids and Surfaces B: Biointerfaces*

Received Date: 4 July 2019

Revised Date: 4 October 2019

Accepted Date: 14 October 2019

Please cite this article as: Boix-Lemonche G, Guillem-Marti J, D'Este F, Manero JM, Skerlavaj B, Covalent grafting of titanium with a cathelicidin peptide produces an osteoblast compatible surface with antistaphylococcal activity, *Colloids and Surfaces B: Biointerfaces* (2019), doi: https://doi.org/10.1016/j.colsurfb.2019.110586

Covalent grafting of titanium with a cathelicidin peptide produces an osteoblast compatible surface with antistaphylococcal activity

Gerard Boix-Lemonche[a]; Jordi Guillem-Marti[b,c]; Francesca D'Este[a]; José María Manero[c]; Barbara Skerlavaj[a,*]

[a]Department of Medicine (DAME); University of Udine; piazzale Kolbe, 4, 33100 Udine; Italy.

[b]Biomaterials, Biomechanics and Tissue Engineering Group, Department of Materials Science and Metallurgical Engineering; Universitat Politècnica de Catalunya (UPC); Av. Eduard Maristany 14, 08930, Barcelona; Spain.

[c]Barcelona Research Center in Multiscale Science and Engineering-UPC; Av. Eduard Maristany 14, 08930, Barcelona; Spain.

*Corresponding author at:

Department of Medicine (DAME); University of Udine; piazzale Kolbe, 4, 33100 Udine; Italy;

e-mail: barbara.skerlavaj@uniud.it

Author's e-mail addresses:

Boix-Lemonche, Gerard: boixlemonche.gerard@spes.uniud.it;

Guillem-Marti, Jordi: jordi.guillem.marti@upc.edu;

D'Este, Francesca: francesca.deste@uniud.it;

Manero, José María: jose.maria.manero@upc.edu;

Statistical Summary

Number of words (including Abstract, Keywords, Introduction, Materials and Methods, Results and Discussion, Conclusions, Notes, Acknowledgements, and Appendix A)	5965
Number of Tables	2
Number of Figures	7

Graphical abstract

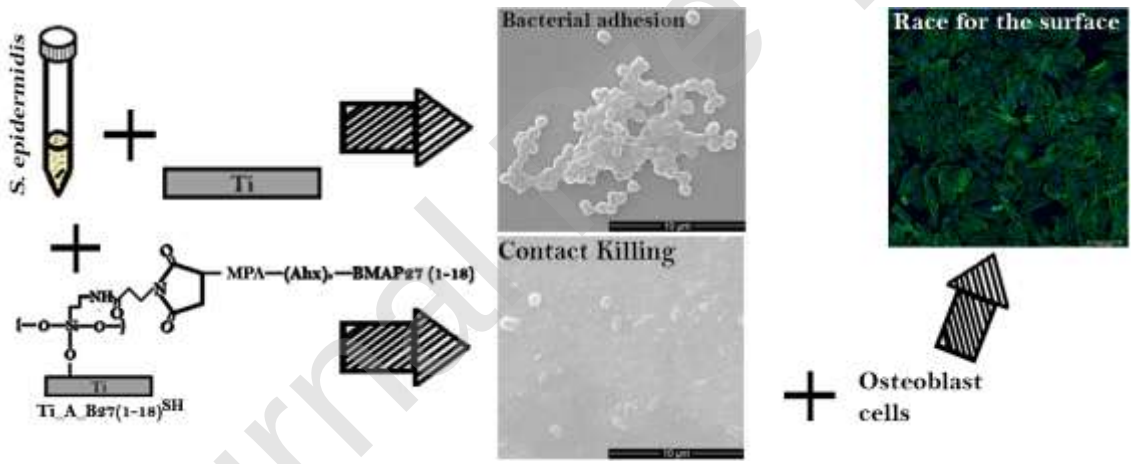

Highlights

- The antimicrobial peptide BMAP27(1-18) was covalently linked to titanium disks
- Staphylococcal adhesion to peptide-modified titanium surface was strongly inhibited
- Bacterial morphology highlighted a bactericidal effect of the anchored peptide
- The tethered peptide was not cytotoxic to osteoblast cells
- Peptide-modified surface improved osteoblast adhesion in co-culture with bacteria

Abstract

Bacterial infection of orthopaedic implants, often caused by *Staphylococcus* species, may ultimately lead to implant failure. The development of infection-resistant, osteoblast-compatible biomaterials could represent an effective strategy to prevent bacterial colonization of implants, reducing the need for antibiotics.

In this study, the widely used biomaterial titanium was functionalized with BMAP27(1-18), an α-helical cathelicidin antimicrobial peptide that retains potent staphylocidal activity when immobilized on agarose beads. A derivative bearing a short spacer with a free thiol at the N-terminus was coupled to silanized titanium disks via thiol-maleimide chemistry. Tethering was successful, as assessed by Contact angle, Quartz Crystal Microbalance with Dissipation monitoring (QCM-D), and X-ray Photoelectron Spectroscopy (XPS), with an average surface mass density of 456 ng/cm^2 and a layer thickness of 3 nm. The functionalized titanium displayed antimicrobial properties against a reference strain of *Staphylococcus epidermidis* with well-known biofilm forming capability. Reduction of bacterial counts and morphological alterations of adhering bacteria, upon 2h incubation, indicate a rapid contact-killing effect. The immobilized peptide was not toxic to osteoblasts, which adhered and spread better on functionalized titanium when co-cultured with bacteria, compared to non-coated surfaces. Results suggest that functionalization of titanium with BMAP27(1-18) could be promising for prevention of bacterial colonization in bone graft applications.

Keywords

Titanium; alpha-helical antimicrobial peptide; biofunctionalization; *Staphylococcus epidermidis*; osteoblasts; osteoblast-bacteria co-culture.

1. Introduction

Infection of implanted prostheses is the most serious complication in arthroplasty procedures and it may lead to implant failure[1]. Treatment is difficult, mainly due to formation of microbial biofilm on device surfaces[1–3]. When sessile, bacteria grow encased in a self-made extracellular matrix that protects them from host defence and renders them less accessible to antibiotics [1,2,4]. Bacteria in biofilms are remarkably less susceptible to currently used antibiotics, when compared to their planktonic counterparts, so that only a few of the available antibiotics are effective against them [3,5,6]. Treatment can be additionally challenging in the case of infections caused by pathogens with acquired antibiotic-resistance [1,5]. Among the most frequent causative agents of prosthetic joint infections and orthopaedic surgical site infections are Gram-positive microorganisms[7], with 20 – 30 % of cases being ascribed to *Staphylococcus aureus* and about 20 – 40 % to coagulase-negative staphylococci[5]. In this respect, *Staphylococcus epidermidis*, which is a harmless commensal in healthy subjects, is emerging as an opportunistic pathogen in immunocompromised patients, preterm newborns, and patients with indwelling medical devices[8]. Its ability to adhere and form biofilm on device surfaces is recognized as a true virulent factor[9].

Consequently, it is crucial to adopt strategies for the prevention of bacterial adhesion to, and biofilm formation on, implant surfaces, not only by improving the perioperative preventative measures but also with the development of osteoblast-compatible biomaterials resistant to bacterial infection. In fact, events following implantation have been described as a “race for the surface”. If it is won by host tissue cells, the implant surface is covered by tissue and becomes less susceptible to bacterial colonization. If, however, it is won by bacteria, then biofilm formation on the implant surface reduces the likeliness of tissue integration[10–12].

Among the several approaches that are currently being examined for orthopaedic applications [13–15], the development of biomaterials coated with antimicrobial peptides

(AMPs) could represent an effective strategy to prevent bacterial colonization of implants[16–18]. AMPs represent an untapped reservoir of natural antibacterial molecules [19,20]. Despite a remarkably high variation in size and sequence, most of these molecules are small, cationic and amphipathic, and are membrane-active[21,22]. Their mode of action, based on membrane permeabilization, has important consequences such as broad spectrum activity including antibiotic-resistant clinical isolates, efficacy also against biofilm-embedded microorganisms, and low tendency to elicit resistance[4,22–24]. These are useful properties in the light of the growing antibiotics resistance problem [25]. Furthermore, various AMPs have been shown to modulate host cell functions in a manner useful for host defence[19], and this includes the bone environment[26–28]. In this respect, several recent studies report the successful tethering of short cationic AMPs onto the surface of titanium (Ti) or other metals by using various coupling procedures [29–37]. These differ mainly by the choice of tethering orientation (N- or C-terminal) and the nature and length of a possible spacer between the peptide and anchoring moiety[16,17,38]. However, there is a lively debate concerning what antimicrobial efficacy is retained by AMPs upon surface anchoring[39–42]. Depending on several parameters related to the structural characteristics of the peptide and to the coupling strategies used for tethering, an immobilized peptide can display quite different antimicrobial properties with respect to its soluble counterpart[43–45]. With respect to covalent surface immobilization, membrane-active peptides could be suitable candidates as they would not need to penetrate into the bacterial cell to reach intracellular targets. Furthermore, assembling short, linear and therefore relatively simple peptide molecules onto a surface should have a positive impact on the production costs.

In a previous study an AMP derived from the α-helical cathelicidin BMAP27, namely the BMAP27(1-18) fragment, was selected for immobilization onto solid support[46]. In solution this peptide displayed potent bactericidal activity against Gram-positive clinical isolates including methicillin resistant *S. aureus* (MRSA)[47,48] and methicillin resistant *S. epidermidis* (MRSE)[46]. It was active also in the presence of relevant biological components such as serum, hyaluronic

acid and synovial fluid, and was biocompatible to osteoblasts[46]. Moreover, an N-biotinylated analogue tethered to streptavidin resin beads retained a potent killing capacity against *S. aureus* and *S. epidermidis*[46].

Based on these properties, in the present study a derivative of BMAP27(1-18) was covalently immobilized on the surface of titanium, which is a widely and routinely used metal for orthopaedic implants[49,50]. Functionalized Ti samples were characterized by contact angle (CA), quartz crystal microbalance with dissipation monitoring (QCM-D) and X-ray photoelectron spectroscopy (XPS). Their antimicrobial efficacy was investigated against a biofilm-forming *S. epidermidis* reference strain by colony forming unit (CFU) counts, evaluation of metabolic activity, and scanning electron microscopy (SEM). Biocompatibility was determined by measuring viability of MG-63 osteoblast-like cells upon cell adhesion to Ti samples. Finally, the capacity to promote cell adhesion also in the presence of contaminating bacteria was addressed in a cell-bacteria co-culture experiment by analysing cell number and morphology by confocal fluorescence microscopy. The aim was to assess whether Ti-immobilized BMAP27(1-18) was able to inhibit bacterial colonization while being compatible with osteoblast cells, with the final goal of exploiting this system for the production of infection-resistant titanium surfaces.

2. Materials and Methods

2.1. Media and reagents.

Polyethylene glycol–polystyrene (PEG-PS) resin, coupling reagents for peptide synthesis and 9-fluorenylmethoxy carbonyl (Fmoc)-amino acids were purchased from Applied Biosystems/Thermo Fisher Scientific (Waltham, MA, USA). Peptide synthesis-grade N,N-dimethylformamide (DMF), dichloromethane, piperidine and high performance liquid chromatography (HPLC)-grade acetonitrile were from Biosolve (Valkenswaard, The Netherlands). Trifluoroacetic acid (TFA) and N-methylmorpholine were from Acros Chimica (Beerse, Belgium). 6-aminohexanoic acid (Ahx) and 3-mercaptopropionic acid (MPA) were purchased from Fluorochem Ltd (Hadfield, Derbyshire, UK).

Commercially pure Ti grade II disks were obtained from Technalloy S.A. (Sant Cugat del Vallès, Spain). (3-aminopropyl)triethoxysilane (APTES) and N-succinimidyl-3-maleimidopropionate (SMP) were purchased from Sigma-Aldrich (St Louis, MO, USA). Alexa fluor 488-phalloidin, Hoechst 33342, and PrestoBlue® reagent were from Invitrogen/Thermo Fisher Scientific. Dehydrated media for antimicrobial activity assays were from Difco laboratories (Detroit, MI, USA), and Oxoid/Thermo Fisher Scientific, cell culture media and supplements from Sigma-Aldrich (St. Louis, MO, USA), and Fetal bovine serum (FBS) from Euroclone (Pero, Italy).

2.2. Sample preparation.

Ti disks of 10 mm diameter and 2 mm height were polished with wet abrasive papers (800, 1200 and 2400 - European P-grade standard) and smoothed with a water suspension of alumina particles (1 µm and 0.05 µm particle size) on cotton cloths. Before the activation and silanization process, samples were ultrasonically rinsed with cyclohexane, isopropanol, distilled water, ethanol and acetone and finally stored dry under vacuum.

2.3. Activation and silanization of samples.

Ti samples were activated by 10 min oxygen plasma treatment at 100 W power in a Standard Plasma System (FEMTO, Diener electronic GmbH, Germany). Samples were silanized with 2 % (v/v) APTES in anhydrous toluene for 1 h at 70 °C under agitation and nitrogen atmosphere. Ti disks were then sonicated for 5 min and washed with toluene, isopropanol, distilled water, ethanol and acetone, and dried with nitrogen. Thereafter, aminosilanized samples were immersed in a 7.5 mM solution of the bifunctional crosslinker SMP in DMF for 1 h under agitation at room temperature. Finally, aminosilanized samples carrying the SMP group (Ti_A) were rinsed with DMF, distilled water, ethanol and acetone, and dried under nitrogen.

2.4. Peptide synthesis.

The amino acid sequence of the α-helical cathelicidin derived peptide BMAP27(1-18) (GRFKRFRKKFKKLFKKLS, amidated C-terminus)[46] was modified at the N-terminus by addition of three aminohexanoic acid (Ahx) residues and one unit of 3-mercaptopropionic acid (MPA) as spacer and anchoring group, respectively. The resulting MPA-$(Ahx)_3$-BMAP27(1-18), hereafter referred to as B27(1-18)^{SH}, was synthesized on a Biotage Initiator+ microwave-assisted automated peptide synthesizer in the solid phase using Fmoc-chemistry, according to published procedures[46]. After cleavage and deprotection, B27(1-18)^{SH} was HPLC-purified and confirmed by mass spectrometry using a Q-STAR hybrid quadrupole time-of-flight mass spectrometer (Applied Biosystems/MDS Sciex, Concord, ON, Canada) equipped with an electrospray ion source. Peptide concentration was determined in aqueous solution by measuring the absorbance at 257 nm taking into account the molar extinction coefficient of 195.1 for each Phe residue[46].

2.5. Immobilization of peptide onto titanium samples.

B27(1-18)^{SH}, dissolved in phosphate buffered saline (PBS) at pH 6.5 to a 100 µM concentration, was deposited onto Ti_A samples (100 µL/disk) and incubated overnight at

room temperature. Thereafter, the peptide functionalized Ti samples were rinsed with PBS and dried with nitrogen. These samples are designated as Ti_A_B27(1-18)^{SH}.

2.6. Physicochemical characterization

2.6.1. Static contact angle measurements and surface energy calculations.

The hydrophilicity of the Ti surfaces was determined by the sessile drop method using the Contact Angle System OCA15 plus (Dataphysics, Filderstadt, Germany). All measurements were done at room temperature using MilliQ ultrapure water (Merck Millipore Corporation, Bedford, MA, USA), and diiodomethane (Sigma-Aldrich, Spain) as wetting liquids (drop volume of 1 µL and 1 µL/min dosing rate). Static contact angles were calculated using SCA 20 software (Dataphysics). The surface energy and its dispersive and polar components were determined using the Owens, Wendt, Rabel, and Kaelble (OWRK) equation applied to both water and diiodomethane measurements [32,51]. Data are means of five measurements per disk for three sample replicates.

2.6.2. X-ray Photoelectron Spectroscopy (XPS).

The chemical composition of the surface of Ti samples was analysed using XPS instrument (D8 advance, SPECS Surface Nano Analysis GmbH, Germany) equipped with an XR50 Mg anode source operating at 150 W and a Phoibos 150 MCD-9 detector. High-resolution spectra were registered with pass energy of 25 eV at 0.1 eV steps at a pressure below 7.5 x 10^{-9} mbar. Binding energies were referenced to the C1s signal. Data were analysed using CasaXPS software (Version 2.3.16, Casa Software Ltd., Teignmouth, UK). Two samples were analysed for each studied condition.

2.6.3. Quartz Crystal Microbalance with Dissipation monitoring (QCM-D).

To quantify and characterize the peptide layer attached to the surfaces, QCM-D measurements were performed on Ti crystal sensors (QSX 310, Q-Sense, Sweden) in a D-300 instrument (Q-sense, Sweden). Ti sensors, cleaned as previously described[52], were activated with O_2 plasma and subsequently treated with APTES and SMP as described

above for Ti_A samples. Prior to monitoring the adsorption of B27(1-18)^{SH}, the baseline was stabilized with PBS for 30 - 60 min. Afterwards, B27(1-18)^{SH} derivative was added (100 µM in PBS, pH 6.5) and changes in resonance frequency and dissipation were monitored at 25 °C for 100 minutes, in real-time using a Qsoft software (Q-Sense, Sweden). Frequency and dissipation curves were fitted to a Voigt viscoelastic model [53] to yield the adsorbed mass and thickness of the peptide layer, as well as kinetic information, by using the Q-tool data analysis software (Q-Sense, Sweden).

2.7. Bacteria and antimicrobial activity assays.

The reference strains *Staphylococcus epidermidis* ATCC 35984, *Staphylococcus aureus* ATCC 25923, *Escherichia coli* ATCC 25922 and *Pseudomonas aeruginosa* ATCC 27853 were used in MIC assays with soluble peptides. Bacteria were cultured either in liquid Brain Hearth Infusion (BHI) (both *Staphylococcus* species) or in Mueller-Hinton (MH) (both Gram-negatives) overnight at 37 °C. *Staphylococcus epidermidis* ATCC 35984 was used in antimicrobial assays with Ti-bound peptide. Stationary phase bacteria were harvested by 10 min centrifugation at 1000 x g and resuspended in sterile PBS (pH 7.4). Bacterial density was assessed by turbidity at 600 nm, with reference to previously determined standards. For the experiments, bacterial suspensions were prepared in MH broth at optimal density.

2.7.1. Determination of the Minimum Inhibitory Concentration (MIC).

The minimum inhibitory concentration (MIC) of B27(1-18)^{SH} in solution was determined by a broth microdilution assay in 96-well microtiter plates, using MH broth with logarithmic-phase microorganisms at 5×10^5 CFU/mL, as previously reported[46], following Clinical and Laboratory Standards Institute (CLSI) guidelines.

2.7.2. Evaluation of bacterial adhesion to titanium surface.

Bacterial adhesion was studied adapting a previously described protocol[33]. Prior to use in antimicrobial assays Ti, Ti_A and Ti_A_B27(1-18)^{SH} samples were sterilized by 30 min treatment with 70 % ethanol, and then thoroughly rinsed with sterile PBS in order to

remove any trace of ethanol. Ti samples were placed in a 24-well plate and incubated with 1 mL of *S. epidermidis* (1 x 10^5 CFU/mL) for 2 h at 37 °C. The medium containing planktonic bacteria was then aspirated and the samples were rinsed three times with sterile PBS. Afterwards, disks were transferred in sterile tubes containing 1 mL of 50 % Mueller-Hinton in sterile PBS (MH-PBS), and adherent bacteria were detached by 10 min vortexing. To make sure that dislodging of bacteria from the surfaces was effective, after the first vortexing step the disks were transferred in new sterile tubes containing 1 mL of MH-PBS and vortexed again for 5 min. Bacterial suspensions from each vortexing step were then serially diluted in MH-PBS and seeded on BHI agar plates. The plates were incubated at 37 °C for 24 h and the resulting colonies counted. All experiments were performed in triplicate for each type of surface.

2.7.3. Scanning Electron Microscopy (SEM).

The morphology of *S. epidermidis* adhered to Ti samples was studied by SEM (Quanta250 SEM, FEI, Oregon, USA) operated in secondary electron detection mode. The working distance was adjusted in order to obtain the suitable magnification; the accelerating voltage was set to 30 kV. SEM was performed in duplicate for each sample. Briefly, upon 2 h incubation as described above, all samples were rinsed three times with filtered sterile PBS, fixed with 2.5 % (v/v) glutaraldehyde for 30 min at 4 °C, rinsed three times with filtered sterile PBS and MilliQ ultrapure water, and dehydrated in graded series of ethanol solutions (20 min each). Immediately prior to SEM analysis, samples were sputter-coated with gold (Sputter Coater K550X, Emitech, Quorum Technologies Ltd, UK).

2.7.4. Bacterial growth kinetics on titanium surfaces.

Ti samples, placed in triplicate into 48-well plates, were immersed in 1 mL of *S. epidermidis* (6×10^4 CFU/mL) suspension in MH for 2 h. The medium containing planktonic bacteria was removed, Ti disks were rinsed with sterile PBS, and adherent bacteria were allowed to grow at 37 °C for 22 h in fresh MH medium supplemented with 10 % (v/v)

PrestoBlue® metabolic dye. Bacterial growth kinetics were monitored fluorometrically according to PrestoBlue® manufacturer's instructions by using a Multimode Plate Reader (EnSpire™ 2300, PerkinElmer, Waltham, MA, USA).

2.8. Cell culture.

The human osteoblast-like MG-63 cell line was obtained from ATCC (Manassas, VA, USA) and maintained in Dulbecco's Modified Eagle Medium (DMEM), in a humidified incubator at 37 °C and 5 % CO_2 atmosphere. DMEM medium was supplemented with 10 % (v/v) heat inactivated FBS, 2 mM L-glutamine, 100 units/mL penicillin and 100 µg/mL streptomycin.

2.8.1. Cell adhesion and viability assay.

The biocompatibility of Ti samples was evaluated by measuring viability of the MG-63 cell line by using the metabolic dye PrestoBlue®. Cells were seeded onto Ti samples in a 48-well plate at a density of 4 x 10^4 cells/well in complete medium and allowed to adhere for 4 h at 37 °C. Thereafter the medium was aspirated, cells were rinsed with sterile PBS and incubated at 37 °C for 90 min in fresh complete medium containing 10 % (v/v) PrestoBlue®. Cell metabolic activity was measured fluorometrically according to PrestoBlue® manufacturer's instructions by using a Multimode Plate Reader (EnSpire™ 2300, PerkinElmer, Waltham, MA, USA). All experiments were performed in triplicate for each type of surface.

2.8.2. Cell-bacteria co-culture.

This assay was performed according to previously reported studies[12,54]. Ti samples were incubated with 1 mL of *S. epidermidis* (6 x 10^4 CFU/mL) in a 48-well plate for 2 h at 37 °C as described above. The medium was then removed and the samples were washed three times in sterile PBS. Next, MG-63 cells, freshly resuspended in DMEM medium without penicillin and streptomycin, supplemented with 2 % MH broth, were seeded on bacteria-covered surfaces at a density of 4 x 10^4 cells/well. Bacteria and MG-63 cells were incubated at 37 °C in humidified 5 % CO_2 for 6 and 24 h. At these time points, samples

were fixed in 3% Paraformaldehyde, stained with Alexa Fluor 488-phalloidin and Hoechst 33342 and examined by Confocal Laser Scanning Microscopy (CLSM) with a Leica TCS SP8 X microscope (Leica Microsystems GmbH, Wetzlar, Germany). Images were analysed using ImageJ 1.51w software (NIH, Bethesda, MD, USA) to determine cell area and surface coverage. All experiments were performed in duplicate for each type of surface.

2.9. Statistical analysis.

Data, presented as mean values ± standard deviations, were analysed by a non-parametric Mann-Whitney U test (IBM SPSS Statistics 20 software, Armonk, NY, USA). Statistical significance was set at *P* value <0.05.

3. Results and Discussion

3.1. Coupling strategy and physicochemical characterization of titanium samples.

The cathelicidin derived peptide BMAP27(1-18), previously shown to possess potent bactericidal activity also upon immobilization on solid support[46], was covalently linked to Ti disks by using the maleimide-thiol chemistry. To this aim, the selected peptide sequence was modified at the N-terminus by adding a spacer and an anchoring moiety bearing a free thiol. The peptide derivative is hereafter referred to as B27(1-18)^{SH}. This modification did not significantly affect the antimicrobial properties of the original peptide, as assessed by determining minimum inhibitory concentration (MIC) against representative Gram-positive and Gram-negative bacterial species (Table 1).

The selected coupling strategy has been previously applied for functionalization of titanium and tantalum with, respectively, the antimicrobial peptide hLF1-11, and the cell adhesive RGD peptide, both for osseointegrative applications[32,33,55]. In the present study this simple and linear functionalization procedure, schematically illustrated in Fig. S1 (see Supplementary material), was used for covalent anchoring of B27(1-18)^{SH} to titanium *via* its N-terminus. Ti disks (Ti) were first treated with oxygen plasma (Ti_Pl) to generate hydroxyl groups required for the subsequent silanization of the metal surface with the aminosilane APTES. The amino group of the organosilane was then exploited to introduce the bifunctional crosslinker SMP, bearing the maleimide function (Ti_A) which was subsequently used to react with the thiol on the peptide N-terminus (Ti_A_B27(1-18)^{SH}) (see Fig. S1 in Supplementary material).

To verify whether the functionalization procedure was successful, Ti samples first underwent physicochemical characterization by static contact angle (CA) measurements and XPS. As expected, CA analysis (Table 2) showed a substantial change in wettability upon

plasma treatment (Ti_Pl *vs*. Ti samples) as well as upon silanization (Ti_A *vs*. Ti_Pl), and subsequent peptide coupling (Ti_A_B27(1-18)^{SH} *vs*. Ti_Pl, and Ti_A_B27(1-18)^{SH} *vs*. Ti_A).

High resolution XPS spectra were then recorded to obtain the chemical composition of the modified Ti surfaces, reported in Fig. 1. Silanization of samples was supported by the presence of silicon (Si 2p) and by the increase in carbon (C 1s) and nitrogen (N 1s) content in Ti_A *vs*. Ti disks. An additional increase of both carbon and nitrogen, and decrease in percent oxygen (O 1s) and titanium (Ti 2p) in Ti_A_B27(1-18)^{SH} samples, with respect to Ti_A disks, indicated stable and strong attachment of peptide molecules to the silanized metal surfaces, thus confirming that the applied procedure for peptide tethering to titanium was both sound and reliable.

The peptide layer formed on the Ti surface was quantified using Quartz Crystal Microbalance with Dissipation monitoring (QCM-D), which is a very sensitive tool to measure masses in the ng/cm^2 range [56]. The technique is based on monitoring the resonance frequency of an appropriate piezoelectric sensor crystal, which decreases proportionally to the adsorbed mass (defined as “adlayer”) on the surface of the crystal itself. The additional monitoring of the dissipation factor enables a more accurate mass estimate by taking into account the contribution of the adsorbed water to the adlayer mass[57].

In the present study, in order to record the formation of a peptide layer covalently linked to titanium, Ti crystal sensors were used and, prior to peptide addition, the surface of the Ti sensor was treated with O_2 plasma, APTES and crosslinker, as described above for Ti disks, and extensively rinsed with PBS. Upon addition of peptide solution, changes in resonance frequency (ΔF, Fig. 2A) and dissipation (ΔD, Fig. 2B) indicated deposition of a stable layer with a rapid drop in ΔF, corresponding to a rapid increase in ΔD, during the first 5 - 6 min. This was followed by stabilization of both parameters during the next 15 – 20 min.

Replacement of the peptide solution by PBS after 80 min monitoring did not result in appreciable modifications of the registered traces, consistent with the formation of a stable peptide monolayer over the silanized surface. By fitting data to the Voigt model[53], an average surface mass density of 456.32 ± 7.61 ng/cm^2 and a layer thickness of 3.08 ± 0.06 nm were determined. Although it is difficult to make direct comparisons, these values are in the same order of magnitude as the QCM-D data obtained by Castellanos *et al.* using cell-adhesive peptides[52] and by Corrales Urena et al. using antimicrobial peptides[58] adsorbed onto CoCr and Ti sensors, respectively. The peptide layer thickness was comparable to that achieved by a basically similar coupling scheme for the antimicrobial peptide Dhvar5 grafted on chitosan[29], and for the covalently bound lactoferrin peptide[33], both determined by ellipsometry. Regarding the surface peptide density on titanium, it is interesting to note that our data are comparable to those obtained by others with colorimetric methods[29,30]. Collectively the physicochemical data support successful functionalization of Ti disks with the cathelicidin peptide derivative B27(1-18)^{SH}.

3.2. Analysis of antimicrobial properties of titanium samples.

The antimicrobial efficacy of Ti-anchored peptide was first tested in terms of bacterial adhesion inhibition. Adhesion of microorganisms to surfaces of implanted biomedical devices is the first and crucial step in bacterial colonization of implants so its prevention should likely prevent the development of infection. Ti samples were exposed to a suspension of *Staphylococcus epidermidis* ATCC 35984, a reference strain with a well-documented biofilm-forming ability[8]. Notably, this feature is considered to be related to the pathogenicity of this otherwise harmless microorganism[2,8]. Bacteria were allowed to adhere to Ti samples for 2 h at 37 °C, then planktonic cells were washed away and surface attached bacteria recovered by a two-step vortexing procedure. As shown in Fig. 3, the colony forming units (CFU) of *S. epidermidis*, recovered from Ti_A_B27(1-18)^{SH} disks, were significantly less than those recovered from both controls, i.e. Ti and Ti_A samples. This

would suggest that bacteria were killed upon contact with the peptide-functionalized Ti, and/or that their adhesion to Ti_A_B27(1-18)^{SH} disks was in some way hindered.

To clarify events occurring at the metal surface during staphylococcal adhesion, the morphology of the attached bacteria was determined by SEM in parallel to CFU counting. As shown in Fig. 4, this analysis revealed a remarkable difference in *S. epidermidis* cells adhered to the different substrata. Bacterial cells on control Ti samples were opaque, round in shape, with smooth surface and with division septa clearly evident (Fig. 4B, 4F). Individual bacteria were on average of the expected size with diameter values ranging from 0.55 μm to 0.85 μm. Dividing microorganisms were very frequent, indicating that bacteria on bare titanium were viable and growing (Fig. 4B, 4F - G). Often several dozens of bacterial cells were clustered together (Fig. 4A, 4C). Such bacterial agglomerates were covered by a dense and grey layer resembling a blanket (Fig. 4A, 4C and 4G). Individual cells were tightly associated with each other and connected by junctions (Fig. 4C, 4E). In addition, in most instances there was a halo surrounding the bacteria at the contact interface between bacterial cell and Ti surface (Fig. 4C, 4G). In some clusters, fimbriae-like surface appendages, connecting bacteria to Ti, were also visible (Fig. 4D - E). All these elements likely represent extracellular matrix components and/or adhesion structures, indicating biofilm initiation [59–61], in line with the well-known biofilm forming properties of *S. epidermidis* ATCC 35984, which is known to be a heavy matrix producer[8,9]. Notably, we did not observe significant morphological differences between bacteria adhered to bare Ti (Ti; Fig. 4A - E) and those adhered to silanized Ti disks (Ti_A; Fig. 4F - G). In contrast to controls, bacteria adhered to Ti_A_B27(1-18)^{SH} samples were not only fewer in number, but also showed dramatically different morphologies (Fig. 4I). They showed increased size and elongated shapes, and division septa were conspicuously missing (Fig. 4J). In addition, bacteria had a knobbly appearance, many were collapsed and deflated and appeared embedded in a layer of amorphous material deposited on the Ti surface (Fig. 4H - J). In many cases, these ghost-

like bacterial cells were surrounded by an empty circle (Fig. 4K), and for some bacteria what appeared to be the extrusion of cytoplasmic material out of the cell was observed (Fig. 4L). Such dramatic changes in morphology pointed to the impairment of microbial cell growth as well as of cell division, which is normally accomplished through formation of the division septum. The observed structures could reasonably derive from dead bacteria. However, the "deflated bag" appearance, in the absence of evident surface lesions such as blebs or holes[62], would suggest that digestion of bacterial content has occurred, possibly upon activation of autolytic enzymes[63].

In Ti_A_B27(1-18)^{SH} samples, the observed changes in morphology matched the reduction in CFUs, thus highlighting killing ability of Ti-immobilized B27(1-18)^{SH}. This finding was not unexpected, considering that BMAP27(1-18) proved able to kill staphylococci when N-terminally anchored to a model support[46]. However, a question arises about its mode of action in the immobilized state. The bactericidal activity of this peptide in solution is based on its ability to perturb microbial membranes, and is intimately related to its ability to adopt an amphipathic conformation[47,64]. In our case however, it appears quite obvious that, presuming their limited mobility, the anchored peptide molecules may interact only with superficial components of the bacterial cell, and thus, the killing action likely differs from that displayed by this type of peptides in solution[47,62,64]. In this respect, it is worth noting that the staphylococci adhered to peptide-functionalized Ti (this study, Fig. 4) were remarkably different from those observed in a previous study after treatment with the sheep cathelicidin SMAP-29 in solution[62]. In this latter case, surface roughening and blebbing of SMAP29-treated microorganisms was interpreted as morphological evidence of the potent permeabilizing activity of this alpha-helical peptide in solution[62], while the bactericidal mode of action of immobilized SMAP-29 [41], or indeed BMAP-27 [65], has not as yet been elucidated.

It is very likely that the negatively charged bacteria were initially attracted by the highly cationic B27(1-18)^{SH} (net charge +10 [46]), but were killed upon their contact/adhesion to the metal, in keeping with what suggested also by other authors[31,44]. The observed changes in morphology could be the result of events triggered by a peptide-induced perturbation at the bacterial surface, as reported for free peptides in solution[63,66,67], and also suggested for immobilized AMPs [44,68].

It is interesting to note however, that in Ti_A_B27(1-18)^{SH} samples, besides dead or heavily damaged bacteria, microcolonies with normal appearance were also occasionally observed (Fig. 4H). This prompted us to investigate whether the surviving bacteria could be able to regrow. To this end, Ti samples were exposed to a suspension of *S. epidermidis* for 2 h as above and, after removal of planktonic microorganisms and washings, the incubation was extended for additional 22 h in fresh MH broth. Since the presence of metal disks in the wells would not allow optical density measurements, growth was kinetically monitored by the PrestoBlue® dye, which emits fluorescence upon conversion by metabolically active microorganisms. As shown in Fig. 5, bacterial growth on control Ti disks (Ti and Ti_A) became detectable at 7 - 8 h post-adhesion, with an exponential phase between 10 - 15 h, and a final plateau at 18 - 20 h. The surviving bacteria on Ti_A_B27(1-18)^{SH} samples showed an about 1.5-h delay both for the beginning of growth and onset of the exponential growth phase, presumably related to their decreased initial number, in keeping with the results of bacterial adhesion assays. Hence, inhibition of the initial bacterial adhesion remains crucial for long lasting antimicrobial efficacy[14].

It is worth stressing in this respect that the experimental conditions used in our *in vitro* assays, such as a relatively high initial inoculum, are likely different from those occurring in clinical settings where a possible bacterial contamination would take origin from a very low bacterial number, as also confirmed by animal model studies[69,70]. In agreement with

what has been suggested by other authors[30], one could reasonably expect a more effective protection under medically relevant conditions, with only few bacteria present at the implant surface thanks to strictly antiseptic surgical procedures.

3.3. Evaluation of compatibility of titanium samples to osteoblast cells.

In the general context of the prosthetic settings, one should take into consideration the complex dynamics of events occurring during and upon implantation, such as osteoblast attachment, growth and differentiation, that collectively should lead to complete implant integration. With this perspective, it was mandatory to assess the biocompatibility of our Ti samples to osteoblast cells. To address this issue, Ti samples were seeded with the osteosarcoma-derived MG-63 cells, used as a model, in a 48-well plate. Adherent cells after 4 h incubation were quantified by a PrestoBlue® metabolic assay. As shown in Fig. 6, metabolic activity of cells on Ti_A and Ti_A_B27(1-18)^{SH} samples was comparable to that of MG-63 cells on bare Ti, which is known for its biocompatibility. This means that cells were vital and able to adhere to various substrata without appreciable toxic effects neither by the peptide nor by other organic molecules present on Ti (e.g. Ti_A). This result adds to previous reports concerning the virtual absence of cytotoxic effects of BMAP27(1-18) against different host cell types, both in solution[47,48,64], and upon immobilization[46].

Given the cytocompatibility of the functionalized Ti samples we next investigated their antimicrobial efficacy in a more complex context by addressing the issue of “race for the surface”. This concept stems from the observation that, in order to achieve successful and long lasting tissue integration of the implanted prosthesis, the surface of an ideal implant should be resistant to bacterial colonization but at the same time prone to colonization by host tissue cells[10,12,71].

To investigate to what extent the colonizing capacity of osteoblast cells might be hampered by bacteria present on Ti itself, a co-culture experiment of MG-63 cells and

bacteria was set up. *S. epidermidis* was allowed to adhere to Ti samples as in the antimicrobial assays described above. After withdrawal of planktonic bacteria and washings, Ti disks contaminated by adherent bacteria were seeded with freshly resuspended MG-63 cells in antibiotic-free DMEM medium supplemented with 2 % MH, and incubated for additional 6 h and 24 h. At these time points, Ti disks were processed and analysed by fluorescence microscopy in order to evaluate MG-63 cell number and morphology.

Data and representative CSLM images are shown in Fig. 7. Data were calculated as percent cell surface coverage respect to bacteria-free Ti controls (Fig. 7A, B), and mean cell area (Fig. 7C, D). It is evident that the presence of bacteria affected cell adhesion and spreading on distinct Ti samples to different extents. For example, at a 6 h time point, osteoblast adhesion to Ti and Ti_A samples was inhibited by about 40 % for bacterial adhered samples, whereas cell adhesion to Ti_A_B27(1-18)^{SH} samples was not impaired but rather enhanced (Fig. 7A). Since at this time point cell size (Fig. 7C) and morphology (Fig. 7, images in the upper row) were on average highly comparable, the increased surface coverage on Ti_A_B27(1-18)^{SH} samples could be reasonably ascribed to a higher number of adhered MG-63 cells. This finding would suggest that the bactericidal action exerted by peptide-functionalized Ti, as observed by SEM (Fig. 5H-L) and confirmed by CFU counts (Fig. 3), was effective enough to allow displacement of bacteria by MG-63 cells, which could thus predominate and spread onto the surface. This hypothesis seems further supported by the increment in both surface coverage (Fig. 7B) and mean cell area (Fig. 7D) observed after 24 h co-incubation on peptide-functionalized samples. However, although BMAP27(1-18) proved neutral with respect to MG-63 cell growth and differentiation in a previous study[46], we cannot exclude specific effects on cells by the Ti-anchored peptide. It is interesting to note that at 24-h time point a slight improvement of cell adhesion and spreading compared to bacteria-free control was observed in Ti and Ti_A samples, which

were devoid of antimicrobial properties (Fig. 3 – 5). This would suggest that besides bacterial killing, one should take into consideration other phenomena in the complex network of multiple interactions between implant surfaces, bacteria, and relevant tissue cells[10,54,72]. In the light of what has been reported for the oral environment[73,74], at present we cannot rule out possible stimulating effects of bacteria on tissue cell expression of adhesion molecules that would in turn improve cell adhesion and spreading.

4. CONCLUSIONS

In order to obtain titanium with anti-infective surface, in this study Ti disks were successfully functionalized with the cathelicidin derived α-helical peptide B27(1-18)^{SH}, as assessed by contact angle, XPS, and QCM-D analyses. Adhesion of *S. epidermidis* to peptide-functionalized samples was markedly reduced and alterations in bacterial morphology revealed by SEM indicate a contact-killing effect of the anchored peptide, suggesting a possibly different mode of action respect to that displayed by this peptide in solution. In this respect, a more profound knowledge of the bactericidal mechanism of surface-immobilized peptide should help design improved peptide derivatives, spacers, and coupling strategies, in order to increase the antimicrobial performance of the functionalized Ti. Importantly, the immobilized peptide did not produce any cytotoxic effect on osteoblast-like cells, which adhered and spread better on functionalized Ti when co-cultured with bacteria compared to non-coated surfaces. For further improvement in view of orthopaedic applications, it would be worth investigating the stability/efficacy of Ti-anchored peptide in the presence of human serum and/or other relevant biological components such as hyaluronic acid, or in the presence of proteases. Although these aspects have not yet been addressed, results obtained in the present study are promising, highlighting the potential of BMAP27(1-18) for the development of biomaterials refractory to microbial contamination.

Notes

The authors declare no competing financial interest.

Acknowledgements

The authors are grateful to Prof. Alessandro Tossi, Department of Life Sciences, University of Trieste, Italy, for peptide synthesis facility and assistance in mass spectrometry, and to Dr. Alessandra Arzese, Department of Medicine, University of Udine, Italy, for helpful discussion. Dr. Davide Porrelli and Dr. Gianluca Turco, Department of Medicine, Surgery and Health Sciences, University of Trieste, Italy, are gratefully acknowledged for technical assistance in SEM analysis.

The authors acknowledge the financial support of departmental research funds (Department of Medicine, University of Udine, Italy). The authors also gratefully thank the Generalitat de Catalunya for funding through project 2017SGR-1165 and the Ministry of Science and Innovation, Spain, for financial support through the MAT2015-67183-R project, cofounded by the EU through the European Regional Development Funds.

Declaration of interests

The authors declare that they have no known competing financial interests or personal relationships that could have appeared to influence the work reported in this paper.

The authors declare the following financial interests/personal relationships which may be considered as potential competing interests:

Appendix A. Supplementary data

Supplementary data associated with this article can be found, in the online version, at “xxxxx”.

References

[1] A.J. Tande, R. Patel, Prosthetic Joint Infection, Clin. Microbiol. Rev. 27 (2014) 302–345. doi:10.1128/CMR.00111-13.

[2] C.R. Arciola, D. Campoccia, P. Speziale, L. Montanaro, J.W. Costerton, Biofilm formation in Staphylococcus implant infections. A review of molecular mechanisms and implications for biofilm-resistant materials, Biomaterials. 33 (2012) 5967–5982. doi:10.1016/j.biomaterials.2012.05.031.

[3] H.O. Gbejuade, A.M. Lovering, J.C. Webb, The role of microbial biofilms in prosthetic joint infections, Acta Orthop. 86 (2015) 147–158. doi:10.3109/17453674.2014.966290.

[4] G. Batoni, G. Maisetta, S. Esin, Antimicrobial peptides and their interaction with biofilms of medically relevant bacteria, Biochim. Biophys. Acta - Biomembr. 1858 (2016) 1044–1060. doi:10.1016/j.bbamem.2015.10.013.

[5] T.F. Moriarty, R. Kuehl, T. Coenye, W.-J. Metsemakers, M. Morgenstern, E.M. Schwarz, M. Riool, S.A.J. Zaat, N. Khana, S.L. Kates, R.G. Richards, Orthopaedic device-related infection: current and future interventions for improved prevention and treatment, EFORT Open Rev. 1 (2016) 89–99. doi:10.1302/2058-5241.1.000037.

[6] M. Taha, H. Abdelbary, F.P. Ross, A. V Carli, New Innovations in the Treatment of PJI and Biofilms—Clinical and Preclinical Topics, Curr. Rev. Musculoskelet. Med. (2018). doi:10.1007/s12178-018-9500-5.

[7] P.C. Matthews, A.R. Berendt, M.A. McNally, I. Byren, Diagnosis and management of prosthetic joint infection, BMJ. 338 (2009) b1773–b1773. doi:10.1136/bmj.b1773.

[8] M. Sabaté Brescó, L.G. Harris, K. Thompson, B. Stanic, M. Morgenstern, L. O'Mahony, R.G. Richards, T.F. Moriarty, Pathogenic Mechanisms and Host Interactions in Staphylococcus epidermidis Device-Related Infection, Front. Microbiol. 8 (2017). doi:10.3389/fmicb.2017.01401.

[9] P.D. Fey, M.E. Olson, Current concepts in biofilm formation of Staphylococcus epidermidis., Future Microbiol. 5 (2010) 917–33. doi:10.2217/fmb.10.56.

[10] A. Gristina, Biomaterial-centered infection: microbial adhesion versus tissue integration, Science (80-.). 237 (1987) 1588–1595. doi:10.1126/science.3629258.

[11] G. Subbiahdoss, R. Kuijer, D.W. Grijpma, H.C. van der Mei, H.J. Busscher, Microbial biofilm growth vs. tissue integration: "The race for the surface" experimentally studied, Acta Biomater. 5 (2009) 1399–1404. doi:10.1016/j.actbio.2008.12.011.

[12] M. Godoy-Gallardo, J. Guillem-Marti, P. Sevilla, J.M. Manero, F.J. Gil, D. Rodriguez, Anhydride-functional silane immobilized onto titanium surfaces induces osteoblast cell differentiation and reduces bacterial adhesion and biofilm formation, Mater. Sci. Eng. C. 59 (2016) 524–532. doi:10.1016/j.msec.2015.10.051.

[13] D. Campoccia, L. Montanaro, C.R. Arciola, A review of the biomaterials technologies for infection-resistant surfaces, Biomaterials. 34 (2013) 8533–8554. doi:10.1016/j.biomaterials.2013.07.089.

[14] J. Gallo, M. Holinka, C. Moucha, Antibacterial Surface Treatment for Orthopaedic Implants, Int. J. Mol. Sci. 15 (2014) 13849–13880. doi:10.3390/ijms150813849.

[15] A.E. Eltorai, J. Haglin, S. Perera, B.A. Brea, R. Ruttiman, D.R. Garcia, C.T. Born, A.H. Daniels, Antimicrobial technology in orthopedic and spinal implants, World J. Orthop. 7 (2016) 361. doi:10.5312/wjo.v7.i6.361.

[16] F. Costa, I.F. Carvalho, R.C. Montelaro, P. Gomes, M.C.L. Martins, Covalent immobilization of antimicrobial peptides (AMPs) onto biomaterial surfaces, Acta Biomater. 7 (2011) 1431–1440. doi:10.1016/j.actbio.2010.11.005.

[17] S.A. Onaizi, S.S.J. Leong, Tethering antimicrobial peptides: Current status and potential challenges, Biotechnol. Adv. 29 (2011) 67–74. doi:10.1016/j.biotechadv.2010.08.012.

[18] M. Riool, A. de Breij, J.W. Drijfhout, P.H. Nibbering, S.A.J. Zaat, Antimicrobial Peptides in Biomedical Device Manufacturing, Front. Chem. 5 (2017) 1–13. doi:10.3389/fchem.2017.00063.

[19] A.T.Y. Yeung, S.L. Gellatly, R.E.W. Hancock, Multifunctional cationic host defence peptides and their clinical applications, Cell. Mol. Life Sci. 68 (2011) 2161–2176. doi:10.1007/s00018-011-0710-x.

[20] G. Wang, B. Mishra, K. Lau, T. Lushnikova, R. Golla, X. Wang, Antimicrobial Peptides in 2014, Pharmaceuticals. 8 (2015) 123–150. doi:10.3390/ph8010123.

[21] L.T. Nguyen, E.F. Haney, H.J. Vogel, The expanding scope of antimicrobial peptide structures and their modes of action, Trends Biotechnol. 29 (2011) 464–472. doi:10.1016/j.tibtech.2011.05.001.

[22] A. Tossi, B. Skerlavaj, F. D'Este, R. Gennaro, Structural and functional diversity of Cathelicidins, in: G. Wang (Ed.), Antimicrob. Pept. Discov. Des. Nov. Ther. Strateg., 2nd ed., CABI, 2017: pp. 20–48. https://lccn.loc.gov/2017016223.

[23] N. Strempel, J. Strehmel, J. Overhage, Potential application of antimicrobial peptides in the treatment of bacterial biofilm infections., Curr. Pharm. Des. 21 (2015) 67–84. http://www.ncbi.nlm.nih.gov/pubmed/25189860.

[24] T. Koprivnjak, A. Peschel, Bacterial resistance mechanisms against host defense peptides, Cell. Mol. Life Sci. 68 (2011) 2243–2254. doi:10.1007/s00018-011-0716-4.

[25] ECDC, European Centre for Disease Prevention and Control. Surveillance of surgical site infections in Europe 2010–2011, 2013. doi:10.2900/90271.

[26] D. Kraus, J. Deschner, A. Jäger, M. Wenghoefer, S. Bayer, S. Jepsen, J.P. Allam, N. Novak, R. Meyer, J. Winter, Human β-defensins differently affect proliferation, differentiation, and mineralization of osteoblast-like MG63 cells, J. Cell. Physiol. 227 (2012) 994–1003.

doi:10.1002/jcp.22808.

[27] M. Kittaka, H. Shiba, M. Kajiya, T. Fujita, T. Iwata, K. Rathvisal, K. Ouhara, K. Takeda, T. Fujita, H. Komatsuzawa, H. Kurihara, The antimicrobial peptide LL37 promotes bone regeneration in a rat calvarial bone defect, Peptides. 46 (2013) 136–142. doi:10.1016/j.peptides.2013.06.001.

[28] Z. Zhang, J.E. Shively, Acceleration of Bone Repair in NOD/SCID Mice by Human Monoosteophils, Novel LL-37-Activated Monocytes, PLoS One. 8 (2013) e67649. doi:10.1371/journal.pone.0067649.

[29] F.M.T.A. Costa, S.R. Maia, P.A.C. Gomes, M.C.L. Martins, Dhvar5 antimicrobial peptide (AMP) chemoselective covalent immobilization results on higher antiadherence effect than simple physical adsorption, Biomaterials. 52 (2015) 531–538. doi:10.1016/j.biomaterials.2015.02.049.

[30] B. Mishra, G. Wang, Titanium surfaces immobilized with the major antimicrobial fragment FK-16 of human cathelicidin LL-37 are potent against multiple antibiotic-resistant bacteria, Biofouling. 33 (2017) 544–555. doi:10.1080/08927014.2017.1332186.

[31] B. Nie, H. Ao, C. Chen, K. Xie, J. Zhou, T. Long, T. Tang, B. Yue, Covalent immobilization of KR-12 peptide onto a titanium surface for decreasing infection and promoting osteogenic differentiation, RSC Adv. 6 (2016) 46733–46743. doi:10.1039/C6RA06778F.

[32] M. Godoy-Gallardo, C. Mas-Moruno, M.C. Fernández-Calderón, C. Pérez-Giraldo, J.M. Manero, F. Albericio, F.J. Gil, D. Rodríguez, Covalent immobilization of hLf1-11 peptide on a titanium surface reduces bacterial adhesion and biofilm formation, Acta Biomater. 10 (2014) 3522–3534. doi:10.1016/j.actbio.2014.03.026.

[33] M. Godoy-Gallardo, C. Mas-Moruno, K. Yu, J.M. Manero, F.J. Gil, J.N. Kizhakkedathu, D.

Rodriguez, Antibacterial properties of hLf1-11 peptide onto titanium surfaces: A comparison study between silanization and surface initiated polymerization, Biomacromolecules. 16 (2015) 483–496. doi:10.1021/bm501528x.

[34] W. Lin, C. Junjian, C. Chengzhi, S. Lin, L. Sa, R. Li, W. Yingjun, Multi-biofunctionalization of a titanium surface with a mixture of peptides to achieve excellent antimicrobial activity and biocompatibility, J. Mater. Chem. B. 3 (2015) 30–33. doi:10.1039/C4TB01318B.

[35] S. Makihira, T. Shuto, H. Nikawa, K. Okamoto, Y. Mine, Y. Takamoto, M. Ohara, K. Tsuji, Titanium Immobilized with an Antimicrobial Peptide Derived from Histatin Accelerates the Differentiation of Osteoblastic Cell Line, MC3T3-E1, Int. J. Mol. Sci. 11 (2010) 1458–1470. doi:10.3390/ijms11041458.

[36] L. Zhou, Y. Lai, W. Huang, S. Huang, Z. Xu, J. Chen, D. Wu, Biofunctionalization of microgroove titanium surfaces with an antimicrobial peptide to enhance their bactericidal activity and cytocompatibility, Colloids Surfaces B Biointerfaces. 128 (2015) 552–560. doi:10.1016/j.colsurfb.2015.03.008.

[37] C.-P. Chen, R.-Y. Jing, E. Wickstrom, Covalent Attachment of Daptomycin to Ti6Al4V Alloy Surfaces by a Thioether Linkage to Inhibit Colonization by Staphylococcus aureus, ACS Omega. 2 (2017) 1645–1652. doi:10.1021/acsomega.6b00567.

[38] N. Masurier, J.-B. Tissot, D. Boukhriss, S. Jebors, C. Pinese, P. Verdié, M. Amblard, A. Mehdi, J. Martinez, V. Humblot, G. Subra, Site-specific grafting on titanium surfaces with hybrid temporin antibacterial peptides, J. Mater. Chem. B. 6 (2018) 1782–1790. doi:10.1039/C8TB00051D.

[39] P. Wadhwani, N. Heidenreich, B. Podeyn, J. Bürck, A.S. Ulrich, Antibiotic gold: tethering of antimicrobial peptides to gold nanoparticles maintains conformational flexibility of

peptides and improves trypsin susceptibility., Biomater. Sci. 5 (2017) 817–827. doi:10.1039/c7bm00069c.

[40] G. Gao, J.T.J. Cheng, J. Kindrachuk, R.E.W. Hancock, S.K. Straus, J.N. Kizhakkedathu, Biomembrane Interactions Reveal the Mechanism of Action of Surface-Immobilized Host Defense IDR-1010 Peptide, Chem. Biol. 19 (2012) 199–209. doi:10.1016/j.chembiol.2011.12.015.

[41] J.W. Soares, R. Kirby, L.A. Doherty, A. Meehan, S. Arcidiacono, Immobilization and orientation-dependent activity of a naturally occurring antimicrobial peptide, J. Pept. Sci. 21 (2015) 669–679. doi:10.1002/psc.2787.

[42] A. Rai, S. Pinto, M.B. Evangelista, H. Gil, S. Kallip, M.G.S. Ferreira, L. Ferreira, High-density antimicrobial peptide coating with broad activity and low cytotoxicity against human cells, Acta Biomater. 33 (2016) 64–77. doi:10.1016/j.actbio.2016.01.035.

[43] M. Bagheri, M. Beyermann, M. Dathe, Mode of action of cationic antimicrobial peptides defines the tethering position and the efficacy of biocidal surfaces, Bioconjug. Chem. 23 (2012) 66–74. doi:10.1021/bc200367f.

[44] K. Hilpert, M. Elliott, H. Jenssen, J. Kindrachuk, C.D. Fjell, J. Körner, D.F.H. Winkler, L.L. Weaver, P. Henklein, A.S. Ulrich, S.H.Y. Chiang, S.W. Farmer, N. Pante, R. Volkmer, R.E.W. Hancock, Screening and Characterization of Surface-Tethered Cationic Peptides for Antimicrobial Activity, Chem. Biol. 16 (2009) 58–69. doi:10.1016/j.chembiol.2008.11.006.

[45] M. Bagheri, M. Beyermann, M. Dathe, Immobilization Reduces the Activity of Surface-Bound Cationic Antimicrobial Peptides with No Influence upon the Activity Spectrum, Antimicrob. Agents Chemother. 53 (2009) 1132–1141. doi:10.1128/AAC.01254-08.

[46] F. D'Este, D. Oro, G. Boix-Lemonche, A. Tossi, B. Skerlavaj, Evaluation of free or

anchored antimicrobial peptides as candidates for the prevention of orthopaedic device-related infections, J. Pept. Sci. 23 (2017) 777–789. doi:10.1002/psc.3026.

[47] B. Skerlavaj, R. Gennaro, L. Bagella, L. Merluzzi, A. Risso, M. Zanetti, Biological Characterization of Two Novel Cathelicidin-derived Peptides and Identification of Structural Requirements for Their Antimicrobial and Cell Lytic Activities, J. Biol. Chem. 271 (1996) 28375–28381. doi:10.1074/jbc.271.45.28375.

[48] M. Benincasa, B. Skerlavaj, R. Gennaro, A. Pellegrini, M. Zanetti, In vitro and in vivo antimicrobial activity of two α-helical cathelicidin peptides and of their synthetic analogs, Peptides. 24 (2003) 1723–1731. doi:10.1016/j.peptides.2003.07.025.

[49] S. Bauer, P. Schmuki, K. von der Mark, J. Park, Engineering biocompatible implant surfaces, Prog. Mater. Sci. 58 (2013) 261–326. doi:10.1016/j.pmatsci.2012.09.001.

[50] A.M. Khorasani, M. Goldberg, E.H. Doeven, G. Littlefair, Titanium in Biomedical Applications—Properties and Fabrication: A Review, J. Biomater. Tissue Eng. 5 (2015) 593–619. doi:10.1166/jbt.2015.1361.

[51] M. Godoy-Gallardo, Z. Wang, Y. Shen, J.M. Manero, F.J. Gil, D. Rodriguez, M. Haapasalo, Antibacterial Coatings on Titanium Surfaces: A Comparison Study Between in Vitro Single-Species and Multispecies Biofilm, ACS Appl. Mater. Interfaces. 7 (2015) 5992–6001. doi:10.1021/acsami.5b00402.

[52] M.I. Castellanos, C. Mas-Moruno, A. Grau, X. Serra-Picamal, X. Trepat, F. Albericio, M. Joner, F.J. Gil, M.P. Ginebra, J.M. Manero, M. Pegueroles, Functionalization of CoCr surfaces with cell adhesive peptides to promote HUVECs adhesion and proliferation, Appl. Surf. Sci. 393 (2017) 82–92. doi:10.1016/j.apsusc.2016.09.107.

[53] F. Höök, B. Kasemo, T. Nylander, C. Fant, K. Sott, H. Elwing, Variations in coupled water, viscoelastic properties, and film thickness of a Mefp-1 protein film during adsorption

and cross-linking: A quartz crystal microbalance with dissipation monitoring, ellipsometry, and surface plasmon resonance study, Anal. Chem. 73 (2001) 5796–5804. doi:10.1021/ac0106501.

[54] B. Zhao, H.C. Van Der Mei, G. Subbiahdoss, J. De Vries, M. Rustema-Abbing, R. Kuijer, H.J. Busscher, Y. Ren, Soft tissue integration versus early biofilm formation on different dental implant materials, Dent. Mater. 30 (2014) 716–727. doi:10.1016/j.dental.2014.04.001.

[55] C. Mas-Moruno, B. Garrido, D. Rodriguez, E. Ruperez, F.J. Gil, Biofunctionalization strategies on tantalum-based materials for osseointegrative applications, J. Mater. Sci. Mater. Med. 26 (2015) 1–12. doi:10.1007/s10856-015-5445-z.

[56] K.A. Marx, Quartz crystal microbalance: A useful tool for studying thin polymer films and complex biomolecular systems at the solution - Surface interface, Biomacromolecules. 4 (2003) 1099–1120. doi:10.1021/bm020116i.

[57] M. Rodahl, B. Kasemo, A simple setup to simultaneously measure the resonant frequency and the absolute dissipation factor of a quartz crystal microbalance, Rev. Sci. Instrum. 67 (1996) 3238–3241. doi:10.1063/1.1147494.

[58] Y.R. Corrales Ureña, L. Wittig, M. Vieira Nascimento, J.L. Faccioni, P.N. Lisboa Filho, K. Rischka, Influences of the pH on the adsorption properties of an antimicrobial peptide on titanium surfaces, Appl. Adhes. Sci. 3 (2015) 7. doi:10.1186/s40563-015-0032-6.

[59] D.L. Williams, R.D. Bloebaum, Observing the Biofilm Matrix of Staphylococcus epidermidis ATCC 35984 Grown Using the CDC Biofilm Reactor, Microsc. Microanal. 16 (2010) 143–152. doi:10.1017/S143192760999136X.

[60] B. Valdez-Salas, E. Beltrán-Partida, S. Castillo-Uribe, M. Curiel-Álvarez, R. Zlatev, M. Stoytcheva, G. Montero-Alpírez, L. Vargas-Osuna, In Vitro Assessment of Early Bacterial

Activity on Micro/Nanostructured Ti6Al4V Surfaces, Molecules. 22 (2017) 832. doi:10.3390/molecules22050832.

[61] P. Cao, Y. Yang, F. Uche, S. Hart, W.-W. Li, C. Yuan, Coupling Plant-Derived Cyclotides to Metal Surfaces: An Antibacterial and Antibiofilm Study, Int. J. Mol. Sci. 19 (2018) 793. doi:10.3390/ijms19030793.

[62] B. Skerlavaj, M. Benincasa, A. Risso, M. Zanetti, R. Gennaro, SMAP-29: a potent antibacterial and antifungal peptide from sheep leukocytes, FEBS Lett. 463 (1999) 58–62. doi:10.1016/S0014-5793(99)01600-2.

[63] M. Wilmes, M. Stockem, G. Bierbaum, M. Schlag, F. Götz, D. Tran, J. Schaal, A. Ouellette, M. Selsted, H.-G. Sahl, Killing of Staphylococci by θ-Defensins Involves Membrane Impairment and Activation of Autolytic Enzymes, Antibiotics. 3 (2014) 617–631. doi:10.3390/antibiotics3040617.

[64] E.K. Lee, Y.-C. Kim, Y.H. Nan, S.Y. Shin, Cell selectivity, mechanism of action and LPS-neutralizing activity of bovine myeloid antimicrobial peptide-18 (BMAP-18) and its analogs, Peptides. 32 (2011) 1123–1130. doi:10.1016/j.peptides.2011.03.024.

[65] K. Rapsch, F.F. Bier, M. Tadros, M. von Nickisch-Rosenegk, Identification of Antimicrobial Peptides and Immobilization Strategy Suitable for a Covalent Surface Coating with Biocompatible Properties, Bioconjug. Chem. 25 (2014) 308–319. doi:10.1021/bc4004469.

[66] A. Müller, M. Wenzel, H. Strahl, F. Grein, T.N. V. Saaki, B. Kohl, T. Siersma, J.E. Bandow, H.-G. Sahl, T. Schneider, L.W. Hamoen, Daptomycin inhibits cell envelope synthesis by interfering with fluid membrane microdomains, Proc. Natl. Acad. Sci. 113 (2016) E7077–E7086. doi:10.1073/pnas.1611173113.

[67] K. Scheinpflug, M. Wenzel, O. Krylova, J.E. Bandow, M. Dathe, H. Strahl, Antimicrobial

peptide cWFW kills by combining lipid phase separation with autolysis, Sci. Rep. 7 (2017) 44332. doi:10.1038/srep44332.

[68] X. Chen, H. Hirt, Y. Li, S. Gorr, C. Aparicio, Antimicrobial GL13K Peptide Coatings Killed and Ruptured the Wall of Streptococcus gordonii and Prevented Formation and Growth of Biofilms, PLoS One. 9 (2014) e111579. doi:10.1371/journal.pone.0111579.

[69] R. Southwood, J. Rice, P. McDonald, P. Hakendorf, M. Rozenbilds, Infection in experimental hip arthroplasties, J. Bone Joint Surg. Br. 67-B (1985) 229–231. doi:10.1302/0301-620X.67B2.3980532.

[70] D. Vidlak, T. Kielian, Infectious Dose Dictates the Host Response during Staphylococcus aureus Orthopedic-Implant Biofilm Infection, Infect. Immun. 84 (2016) 1957–1965. doi:10.1128/IAI.00117-16.

[71] V.T.H. Pham, V.K. Truong, A. Orlowska, S. Ghanaati, M. Barbeck, P. Booms, A.J. Fulcher, C.M. Bhadra, R. Buividas, V. Baulin, C.J. Kirkpatrick, P. Doran, D.E. Mainwaring, S. Juodkazis, R.J. Crawford, E.P. Ivanova, "Race for the Surface": Eukaryotic Cells Can Win, ACS Appl. Mater. Interfaces. 8 (2016) 22025–22031. doi:10.1021/acsami.6b06415.

[72] K.G. Neoh, X. Hu, D. Zheng, E.T. Kang, Balancing osteoblast functions and bacterial adhesion on functionalized titanium surfaces, Biomaterials. 33 (2012) 2813–2822. doi:10.1016/j.biomaterials.2012.01.018.

[73] M. Engels-Deutsch, S. Rizk, Y. Haïkel, Streptococcus mutans antigen I/II binds to α5β1 integrins via its A-domain and increases β1 integrins expression on periodontal ligament fibroblast cells, Arch. Oral Biol. 56 (2011) 22–28. doi:10.1016/j.archoralbio.2010.08.010.

[74] P.R. Kramer, A. JanikKeith, Z. Cai, S. Ma, I. Watanabe, Integrin mediated attachment of periodontal ligament to titanium surfaces, Dent. Mater. 25 (2009) 877–883.

doi:10.1016/j.dental.2009.01.095.

Figure captions

Fig. 1. Chemical composition (atomic percentage) obtained by XPS analysis of the indicated titanium surfaces. Results are the average ± SD of at least two samples for each condition.

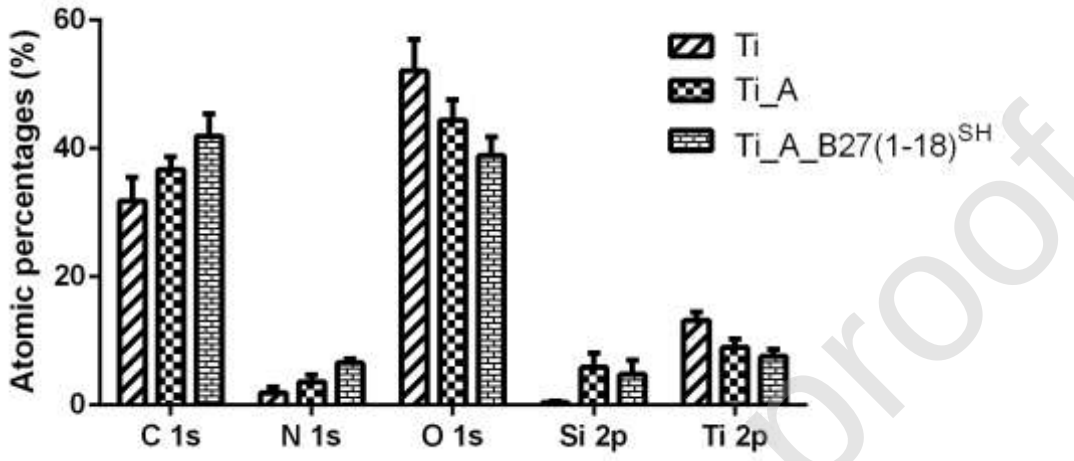

Fig. 2. Resonance frequency (A) and dissipation (B) of a Ti crystal sensor upon addition of B27(1-18)^{SH} solution in a QCM-D assay. Prior to addition of 100 μM peptide solution in PBS, the sensor has been treated as described in Materials and Methods. Data were fitted in the Voigt viscoelastic model to obtain surface mass density and thickness values.

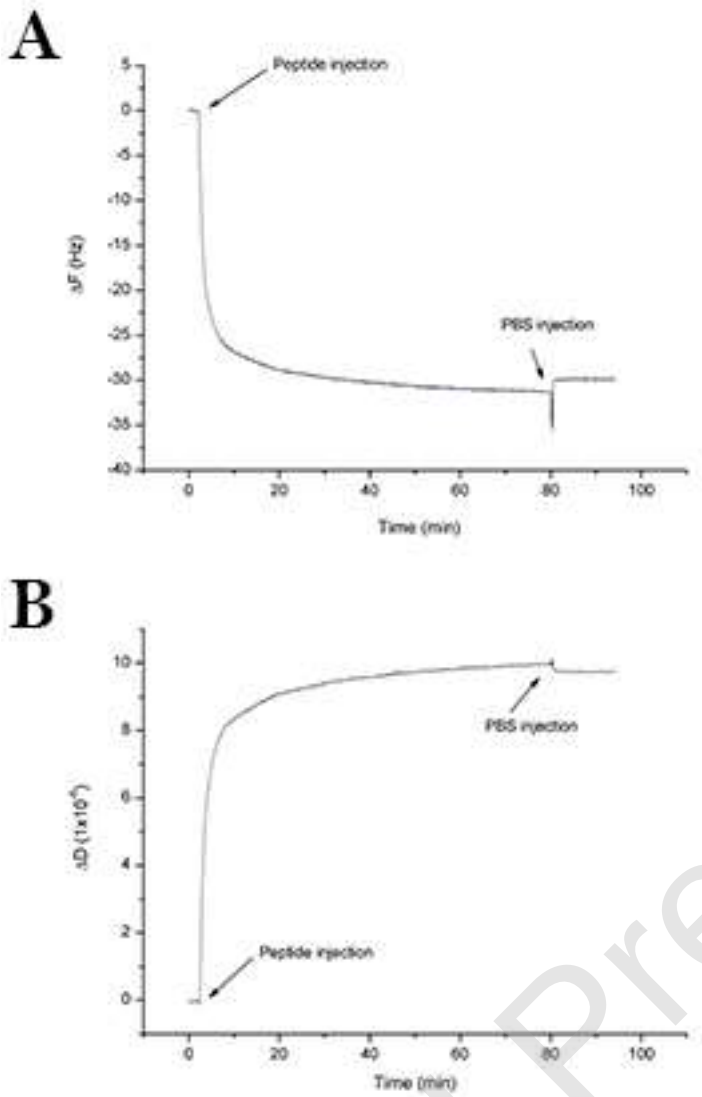

Fig. 3. Adhesion of *S. epidermidis* to the indicated Ti samples. Following 2 h incubation at 37 °C, the CFUs of adherent microorganisms were recovered by a vortexing procedure, serial dilutions and plating on solid medium. Results are expressed as percent CFU respect to CFU recovered from bare titanium (Ti) and are the means ± SD of at least three independent experiments performed in triplicate. * Statistically significant difference *vs*. Ti and *vs*. Ti_A ($P < 0.05$).

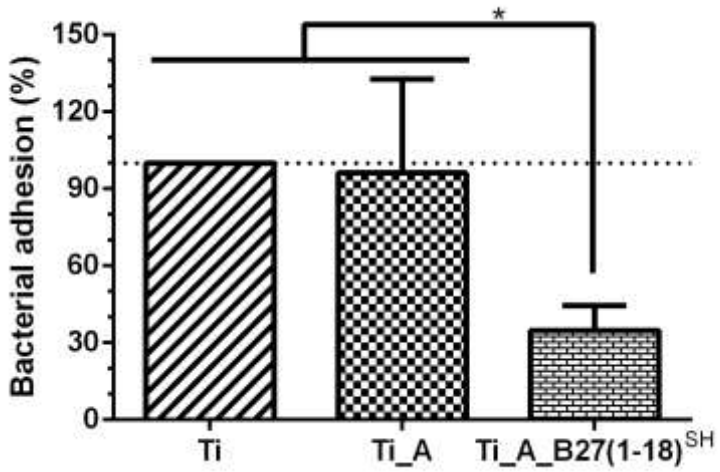

Fig. 4. Morphology of *S. epidermidis* on distinct titanium samples analyzed by SEM. Upon 2 h incubation all samples were rinsed, fixed and processed for SEM analysis. Panels A – E, Ti; panels F – G, Ti_A; panels H – L, Ti_A_B27(1-18)^{SH}. Panel E is a higher magnification of the image represented in Panel A. Arrows indicate, respectively, division septa (▲), contact junctions ( ), halos ( ), pseudopod-like structures ( ), empty circles ( ), extruded cytoplasmic material ( ). Representative images from two experiments performed in duplicate are shown.

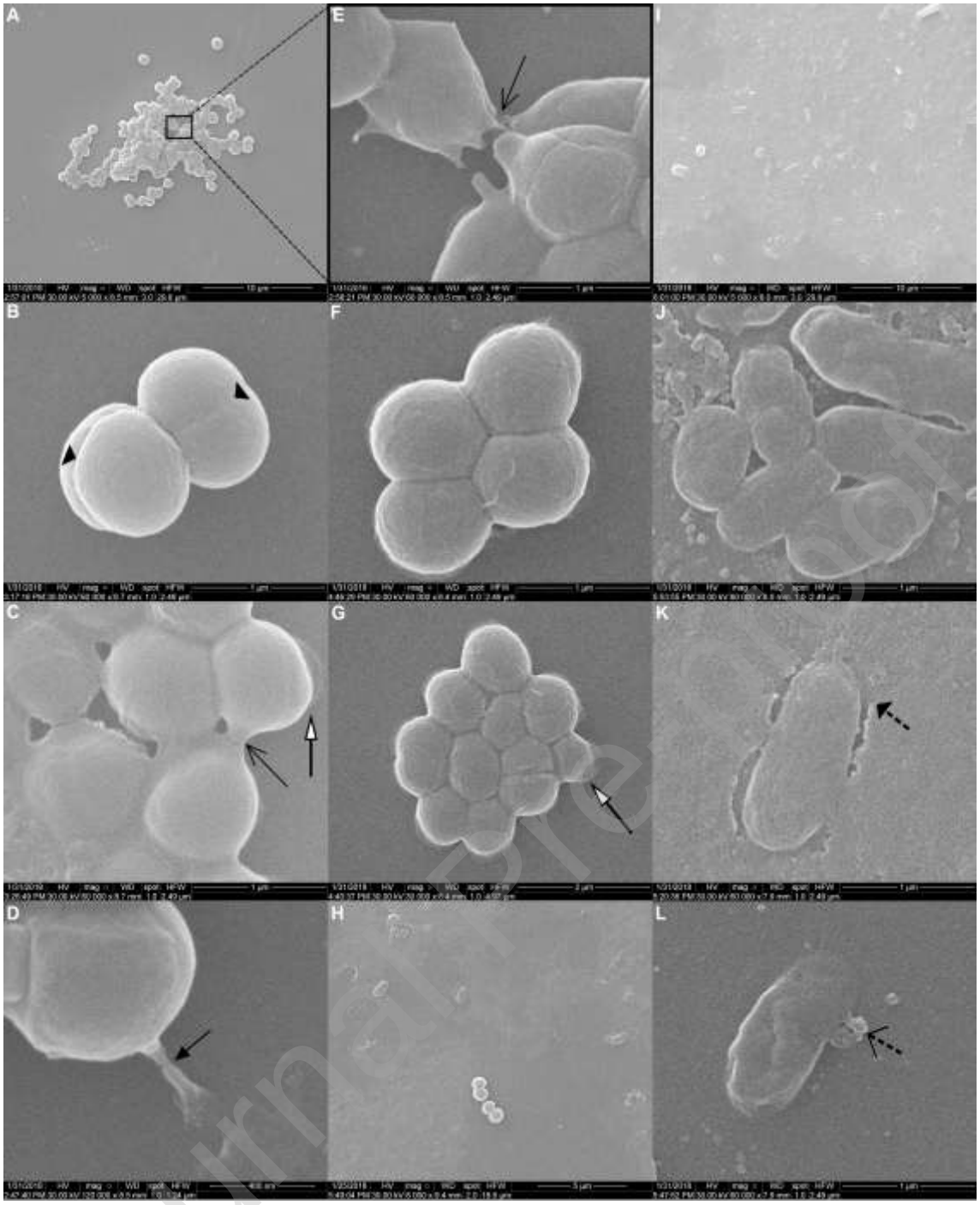

Fig. 5. Growth kinetics of *S. epidermidis* on the indicated Ti samples (Ti, circles; Ti_A, squares; Ti_A_B27(1-18)^{SH}, triangles). After 2 h incubation and washing, fresh MH supplemented with the metabolic dye PrestoBlue® was added and adherent bacteria were allowed to grow overnight at 37 °C. Growth kinetics were monitored by measuring fluorescence emission that is directly proportional to microorganism

viability. Results are reported as relative fluorescence units (RFU) and are the means ± SD of at least three independent experiments performed in triplicate.

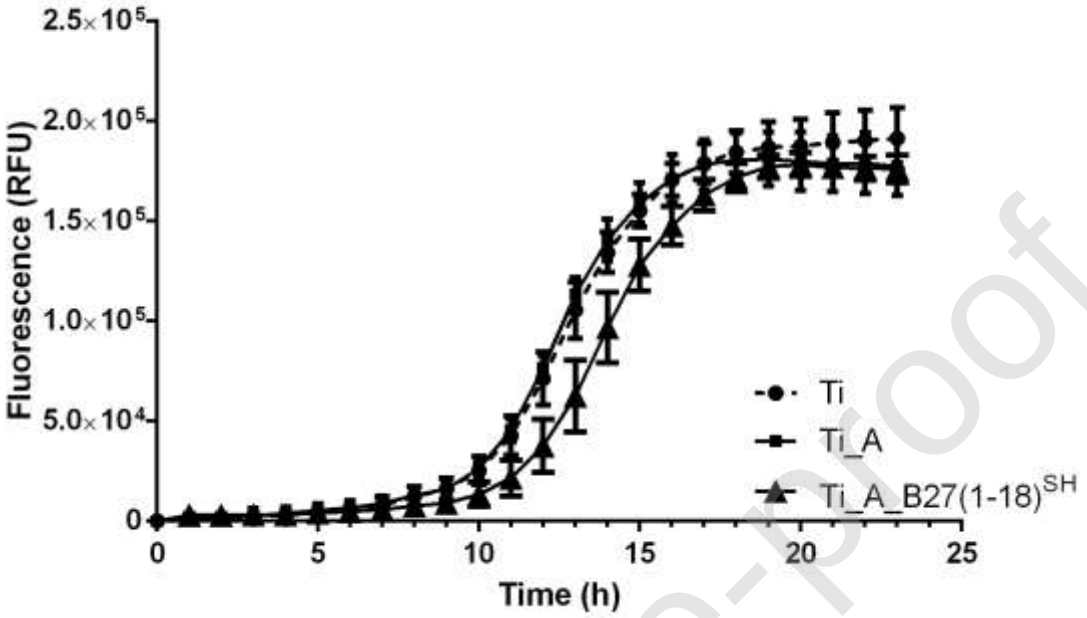

Fig. 6. Osteoblast viability upon adhesion to functionalized Ti samples. MG-63 osteoblast cells were seeded on Ti disks in a 48-well plate in complete medium. After 4 h incubation samples were gently washed and viability of adherent cells quantified by the metabolic dye PrestoBlue®. Results are expressed as percent cell viability respect to cells seeded on bare titanium and are the means ± SD of at least three independent experiments performed in triplicate. Differences between samples did not reach statistical significance.

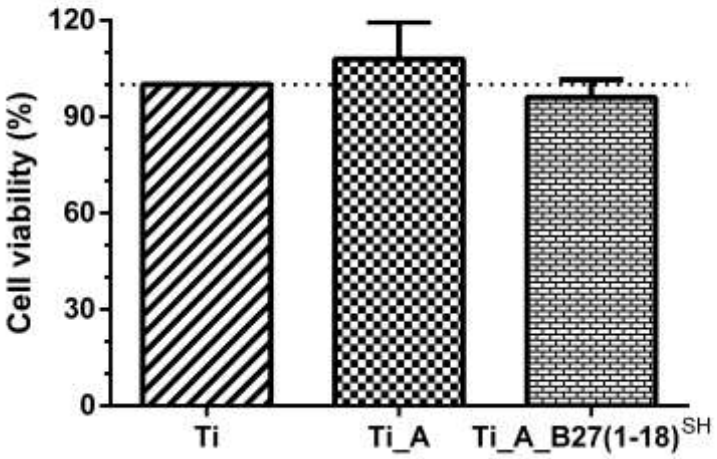

Fig. 7. Osteoblast adhesion to the indicated Ti samples in a cell-bacteria co-culture experiment. MG-63 cells were seeded on functionalized Ti disks, previously incubated with *S. epidermidis*, and co-cultured in antibiotic-free medium for additional 6 h (A, C) and 24 h (B, D). At these time points, samples were fixed and stained with Alexa Fluor 488-phalloidin and Hoechst. Osteoblast cell number and morphology were evaluated by CLSM with a Leica TCS SP8 X microscope followed by quantification with the ImageJ software. Results are expressed as means ± SD of five optical fields for each condition on duplicate samples. A, B: percent cell surface coverage in the presence of bacteria respect to bacteria free controls. C, D: mean cell area values in the presence (Ti, Ti_A, Ti_A_B27(1-18)^{SH}) and in the absence (Ti_cells) of bacteria. Asterisks denote statistically significant differences between the indicated samples ($P < 0.05$). Representative images for each condition are shown in the lower part of the figure. Scale bar = 100 μm.

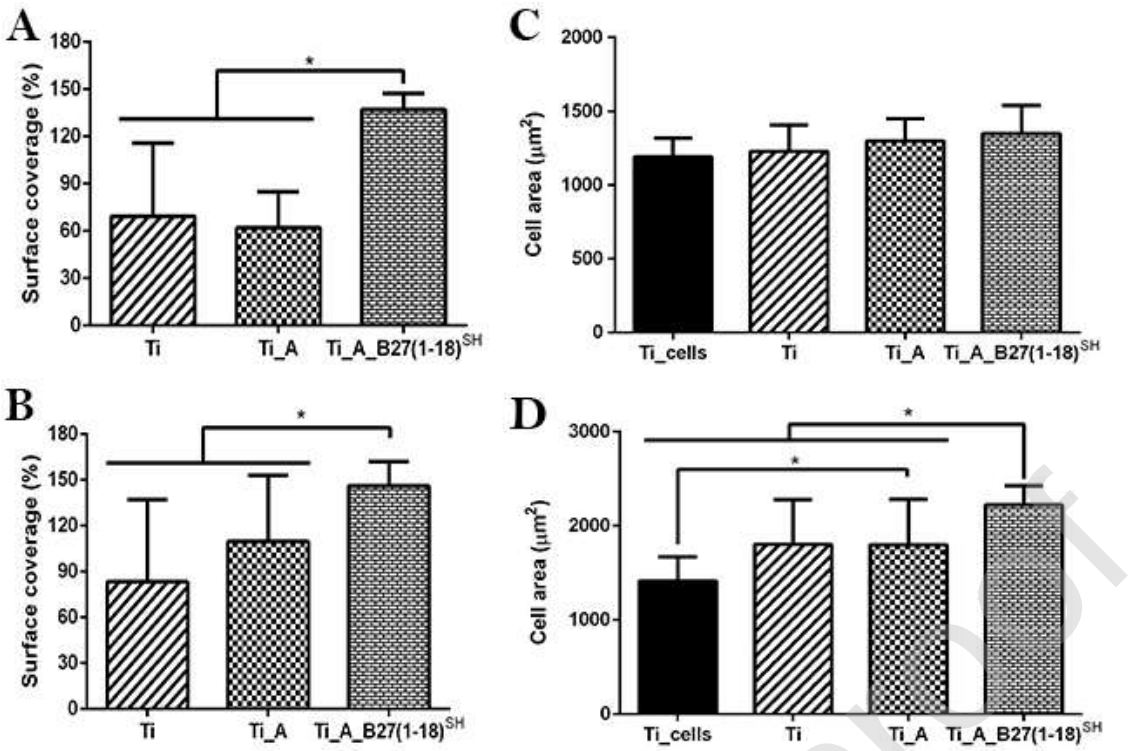

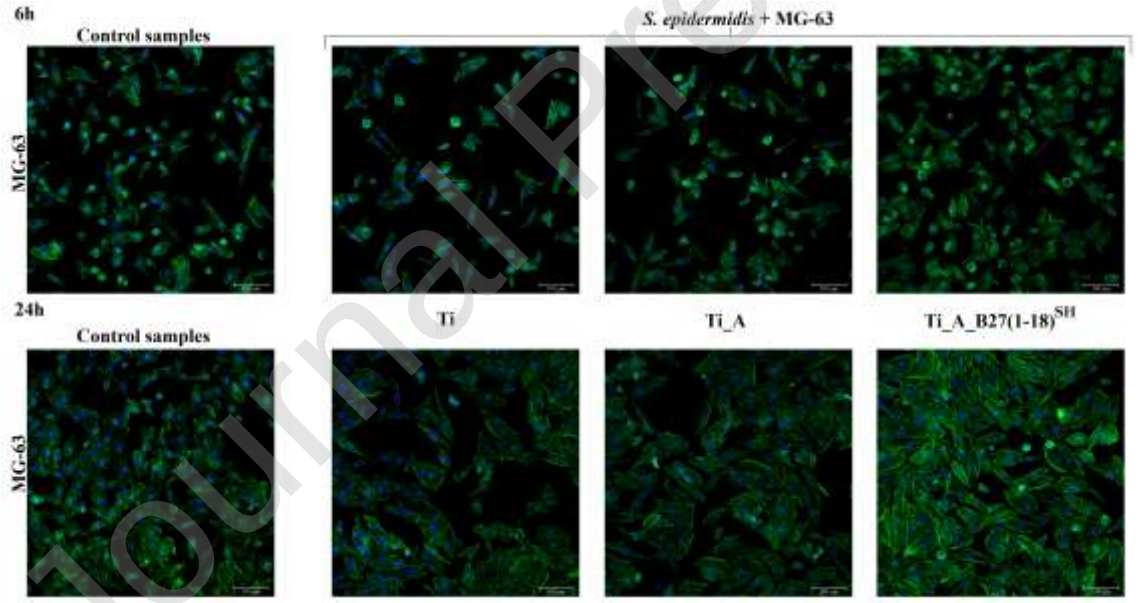

Table 1. Antimicrobial activity of soluble peptides against reference strains

	BMAP27(1-18)	B27(1-18)^{SH}
	MIC (μM)[a,b]	
S. epidermidis ATCC 35984	2	1
S. aureus ATCC 25923	4	4
E. coli ATCC 25922	2	4
P. aeruginosa ATCC 27853	2	4

[a] Determined in MH broth

[b] Data are means of at least 3 independent experiments.

Table 2. Contact angle values and calculation of surface free energy and of its polar and dispersive components. Results are expressed as means ± SD of five measurements for each condition on duplicate samples.

	CA_w (°)	**POL (mJ/m^2)**	**DISP (mJ/m^2)**	**SFE (mJ/m^2)**
Ti	70.4 ± 0.5	8.0 ± 0.3	37.0 ± 0.2	45.1 ± 0.2
Ti_Pl	7.5 ± 0.2 [a]	32.4 ± 0.1 [a]	46.5 ± 0.1 [a]	78.9 ± 0.1 [a]
Ti_A	62.7 ± 0.9 [a,b]	12.0 ± 0.5 [a,b]	36.8 ± 0.5 [b]	48.9 ± 0.6 [a,b]
Ti_A_B27(1-18)^{SH}	68.3 ± 0.9 [b,c]	8.6 ± 0.4 [b,c]	38.4 ± 0.5 [a,b]	47.0 ± 0.6 [a,b]

CA_w: contact angle water; POL: polar component; DISP: dispersive component and SFE: surface free energy.

[a] Statistically significant differences versus control Ti ($P < 0.05$).

[b] Statistically significant differences vs. Ti_Pl ($P < 0.05$).

[c] Statistically significant differences vs. Ti_A ($P < 0.05$).